

Topology Inference for Multi-agent Cooperation under Unmeasurable Latent Input

Qing Jiao[†], Yushan Li[†], Jianping He[†] and Ling Shi[‡]

Abstract—Topology inference is a crucial problem for cooperative control in multi-agent systems. Different from most prior works, this paper is dedicated to inferring the directed network topology from the observations that consist of a single, noisy and finite time-series system trajectory, where the cooperation dynamics is stimulated with the initial network state and the unmeasurable latent input. The unmeasurable latent input refers to intrinsic system signal and extrinsic environment interference. Considering the time-invariant/varying nature of the input, we propose two-layer optimization-based and iterative estimation-based topology inference algorithms (TO-TIA and IE-TIA), respectively. TO-TIA allows us to capture the separability of global agent state and eliminates the unknown influence of time-invariant input on system dynamics. IE-TIA further exploits the identifiability and estimability of more general time-varying input and provides an asymptotic solution with desired convergence properties, with higher computation cost compared with TO-TIA. Our novel algorithms relax the dependence of observation scale and leverage the empirical risk reformulation to improve the inference accuracy in terms of the topology structure and edge weight. Comprehensive theoretical analysis and simulations for various topologies are provided to illustrate the inference feasibility and the performance of the proposed algorithms.

I. INTRODUCTION

Cooperative control has received considerable attention in the last decades, related to a broad range of applications, such as formation control, flocking, and distributed sensor networks [2]–[4]. Among these applications, rich dynamical behavior is emerged from the interactions among the connected agents, as they can share information to achieve agreement on the specific quantities of interest to adapt environment changes. Therefore, the interaction topology, which encodes the key information about network structure and agent communication, plays a crucial role in multi-agent cooperation.

However, the real interaction topology is always unavailable [5] and has to be inferred from the dynamic process in many real-world networks, e.g., gene regulatory networks [6], social networks [7], transportation networks, and computer networks [8]. To learn the real interaction topology, which commonly refers to topology inference, is a crucial cornerstone and fundamental step for a deeper understanding of multi-agent cooperative control.

[†]: Qing Jiao, Yushan Li and Jianping He are with the Department of Automation, Shanghai Jiao Tong University, and Key Laboratory of System Control and Information Processing, Ministry of Education of China, Shanghai, China (e-mail: {jiaoqing, yushan_li, jphe}@sjtu.edu.cn).

[‡]: Ling Shi is with the Department of Electronic and Computer Engineering, Hong Kong University of Science and Technology, Hong Kong, China (e-mail: eesling@ust.hk).

Preliminary results have been submitted to IEEE American Control Conference 2021 [1].

A. Motivations

There are plenty of works that infer the network topology from the observations of various dynamical models in recent years. Despite the prominent contributions of all these pioneering works, there remain three notable unresolved issues. First, many existing works about topology inference only consider undirected networks, which implies that the weight interaction matrix is symmetrical. This property brings simplicity and tractability for mathematical analysis, but is difficult to generalize to directed cases. Second, most network models are proposed with specific signals (e.g., initial agent state [7], external input [9], [10], and intrinsic noise [11]), with the assumption that some prior statistical characteristics of these signals are known. Nevertheless, such model assumptions have less real physical meanings or are unavailable in many practical cases. For example, when the initial network state is uncontrollable, or the system stimulus is unmeasurable, the correlations between agents could be submerged [12]. Third, to meet the accuracy requirement, some additional constraints are needed, e.g., the number of sample process [13], network size [14], or the length of a single sample [15] which should be large enough. Despite the favorable analytic properties brought by these constraints, they limit or even prevent the use of existing methods from inferring more realistic and complex networks, e.g., partially observable networks, or networks whose sizes change dynamically. To resolve these issues simultaneously, more efficient methodologies should be developed to accommodate asymmetric topology and relax the dependence on the prior knowledge of the system dynamics.

Three aspects of the cooperation process inspired our methods. First, the dataset associated with a dynamic process is typically an abstract descriptor of interaction topology. There have been a variety of studies that learn the network topology from underlying data, in which some common features of the network are contained, e.g., graph sparsity [16] and signal smoothness [17]. Second, inference accuracy is closely related to the observation scale. Although using more observations brings more benefits to the estimation result, it also incurs higher computation cost. Thus, it is meaningful to improve the inference accuracy while using as few observations as possible. Third, the latent input, which represents the unknown intrinsic stimulus and the unpredictable extrinsic interference, is commonly injected into the network in the practical dynamic process. Such additional signals are necessary for multi-agent in the distributed inference [18], which inspires us to model the cooperation dynamics under the latent input. In general, latent inputs are classified by the time-property, i.e., time-invariant inputs and time-varying inputs. Time-invariant inputs refer to the physical static variables, e.g., the vector of bus voltage

magnitudes and the branch current in the smart grid [19]. Time-varying inputs refer to dynamic variables with wider applications, e.g., linear false injection [20], malicious jamming attack [21], and micro-incremental transmission losses [22]. This kind of classification helps simplify the theoretical analysis and reduce the complexity of solving optimization-based topology inference problems.

All the above observations motivate us to investigate the topology inference for more general weighted directed networks, while without prior information of the network dynamics, latent input and constraints on the dynamic process. Our work is of theoretical and practical significance, and it will be achieved by an improved reformulation of the optimization problem and an iterative estimation strategy.

B. Contributions

In this paper, we propose a two-layer optimization-based topology inference algorithm (TO-TIA) towards the time-invariant input and an iterative estimation-based topology inference algorithm (IE-TIA) towards the time-varying input. The major challenges of topology inference lie in three aspects. First, the time-invariant/varying property of latent input is unknowable to external observation, making it difficult to formulate the inference model exactly. Second, the observed states of agents are a coupled reflection of the initial system state and latent input, bringing a harsh obstruction to separate the two distinct influences. Third, the performance of topology inference relies heavily on the amount of observations, further requiring more advanced algorithm to improve the inference accuracy, especially when only the partial period of a single dynamic process is observable.

The differences between this paper and its conference version [1] include i) the time-varying input is considered to model more general application scenarios, ii) the two-layer optimization is designed to reduce the computation burden, and iii) the latent input is identified to further improve the inference accuracy. The main contributions of this work are summarized as follows:

- We contribute to the multi-agent cooperation research by revealing the feasibility to infer the directed interaction topology under the unmeasurable latent input, without the prior knowledge about system dynamics and additional conditions about the observation process.
- TO-TIA is proposed to eliminate the unknown influence of time-invariant input on the agent state, and improve the inference accuracy by a two-layer optimization strategy. IE-TIA is proposed to extract the time-varying input directly from the agent state, and improve the inference accuracy by an iterative estimation strategy. Both the algorithms relax the dependence of inference accuracy on observation scale with different computation cost.
- We analyze the feasibility of using the proposed algorithms for topology inference, and evaluate algorithm performance in terms of the accuracy of topology structure and network edge weight. Extensive simulations demonstrate the effectiveness of the proposed algorithms.

The theoretical results in this paper provide a significant step towards more practical applications. TO-TIA and IE-TIA

TABLE I
IMPORTANT NOTATIONS

Symbol	Definition
K	the number of observations
P	the interaction matrix
\mathbf{u}	the latent input
ε	the sampling period
\mathbf{z}	the agent state
\mathbf{z}_0	the part of \mathbf{z} generated by initial state
\mathbf{z}_u	the part of \mathbf{z} generated by latent input
\mathbf{z}_φ	the data in which latent input is filtered
ψ_s	the structure error
ψ_m	the magnitude error
ψ_θ	the parameter error
ψ_d	the magnitude difference
k_{uj}	the injection time for agent j
l	the maximum Lipschitz constant
$\{\alpha_k\}$	the weight setting for objective function

are useful to i) learn the interactions between the interesting agents and predict the agent state update, ii) capture the actual geometry of the physical structure in the nature, and iii) detect the structural error and potential attack during the practical dynamic process.

C. Organization and Notations

The remainder of this paper is organized as follows. Related work is reviewed in Section II. Section III introduces the necessary preliminaries and describes the problem of interest. Section IV develops the first algorithm TO-TIA. Section V develops the second algorithm IE-TIA. Simulation results are shown in Section VI. Section VII concludes this paper. All the proofs of the main results are provided in the Appendix.

Notation: The script \sim and $\hat{\cdot}$ right above a variable represent its corresponding observation and estimation value, respectively, and the parenthesized superscript (i) denotes the i -th iteration. All sets are expressed in calligraphy letters, all matrices are expressed in capital letters, and all vectors are expressed in bold lowercase letters. The row of the matrix X , the entry of the matrix X , and the entry of the vector \mathbf{x} are denoted by $X_{[i]}$, X_{ij} , and x_i , respectively. $\mathbf{0}$, $\mathbf{1}$, and I refer to all-zero column vector, all-one column vector, and identity matrix, respectively. $Z^{k_1:k_2}$ represents the matrix whose columns consist of the vector $\mathbf{z}(k)$ in the time interval $[k_1, k_2]$. The important notations are given in TABLE I.

II. RELATED WORKS

Topology inference is an inverse problem from a pure mathematical view. A brief overview of some representative works is as follows.

There has been extensive research on topology inference for various dynamical models. On the one hand, graph signal processing (GSP) approaches have been proposed, which offer a new perspective on the problem of topology inference from the observed signals [33]. The approaches leveraging GSP

tools usually model observations as graph signals and model dynamic process as the description of a physical system. This kind of models are mainly based on three aspects [34]: signal smoothness [35], causal dependency [36], [37], and network diffusion [38], [39]. Among these GSP-based methods, assumptions on the structure of network and the properties of signals play an important role in determining the performance of the inference results, e.g., the sparsity of networks [40] and the smooth of signals [41]. On the other hand, data-driven approaches [42], [43] have been proposed to determine the underlying structure and the parameters of dynamical systems. In the model constructed by data-driven approaches, each node represents a random variables and the network structure between them reflects conditional dependencies. A classic approach to learn the topology from data is to use a sequential system identification and compute the desired topology using the estimated model. Data-driven methods require some prior knowledge of dynamical systems, e.g., the eigenvalue-eigenvector pair of the adjacent matrix is known [9], and the interaction kernel is Lipschitz [13]. With no prior knowledge of the system, Yuan *et al.* [24] revealed the feasibility of identifying the system from data.

Among different kinds of dynamical systems, the consensus is a fundamental tool to support efficient information exchange, e.g., the convergence speed and stability. This is due to its analytic tractability and simplicity in approximating the fundamental behaviors [10]. Focusing on the consensus dynamics, many methods have been developed across different fields, including node knockout [44], synchronization-based technique [45], spectral density measurement [46], interaction geometry learning [47], and correlation methods [14], [48]. When it comes to improving the inference precision from the consensus-like dynamics, the optimization-based strategies [49], [50] have been proposed, which provide an effective way to solve the easier inference problems with lower communication complexity. Furthermore, in more practical applications, the communication between agents changes dynamically (e.g., interaction links between agents are unreliable [51]), which leads to switching network topology. If the shared information keeps exchanged during the cooperation process, the local neighbors of each agent will also change over time. [52] investigated consensus problem in the directed network with switching topology, and many optimization models [53], [54] have been built to reconstruct the sparsely connected dynamical network based on the eigenvalue decomposition.

Our work is closely related to the extensive literature on GSP-based methods, and provides a new perspective to address the considered issues. Instead of relying on the specific assumptions on the system dynamics or the prior knowledge of the network, we investigate a more general weighted directed network, thus extending the topology inference to more practical consensus-based cooperative control. Besides, the proposed algorithms enable us to obtain sufficiently precise estimation under limited observations.

III. PRELIMINARIES AND PROBLEM DESCRIPTION

A. Preliminaries

Graph and Matrix Theory: Let $\mathcal{G}(\mathcal{V}, \mathcal{E})$ be a directed connected graph which models the communication topology among N agents, where $\mathcal{V} = \{1, \dots, N\}$ is the set of N agents and $\mathcal{E} \subseteq \mathcal{V} \times \mathcal{V}$ is the set of edges. The edge $(i, j) \in \mathcal{E}$ is associated with the weight a_{ij} , and $a_{ij} \neq 0$ indicates that agent i receives information from agent j . The agent set $\mathcal{N}_i = \{j | a_{ij} \neq 0, j \in \mathcal{V}\}$ consists of all the neighbors of agent i , the adjacency matrix $A = [a_{ij}]_{i,j=1}^N$ is an asymmetric matrix consisting of all the edge weights, and the diagonal matrix is defined as $D = \text{diag}(A\mathbf{1})$. The Laplacian matrix is defined as $L = D - A$. Let $L = VJV^{-1}$ be the Jordan decomposition of L , where V and V^{-1} are the matrices whose columns are the left and right eigenvectors of L , respectively, and $J = \text{diag}(J_i)$ with J_i being the Jordan block of eigenvalue λ_i . Define \mathbf{v}_i and \mathbf{w}_i as the column vector of V and V^{-1} , respectively, and in combination with the eigenvalue decomposition, we have

$$(\lambda_i I - L)\mathbf{v}_i = \mathbf{0}, \quad \mathbf{w}_i^T (\lambda_i I - L) = \mathbf{0}, \quad (1)$$

and $\mathbf{w}_i^T \mathbf{v}_j = 0$ ($i \neq j$). For ease of exposition, we order the eigenvalues as $0 = |\lambda_1| < |\lambda_2| \leq \dots \leq |\lambda_N|$, let $\mathbf{v}_1 = \mathbf{1}$, and normalize $\mathbf{w}_i^T \mathbf{v}_i = 1$ for $i = 1, \dots, N$.

Continuous-time Dynamical Model. A general consensus-based cooperation protocol [23] with latent input is

$$\dot{z}_i(t) = \sum_{j \in \mathcal{N}_i} a_{ij}(z_j(t) - z_i(t)) + u_i(t), \quad (2)$$

where $z_i(t)$ is the state of agent i , and $u_i(t)$ is the latent input injected into the network via agent i . Based on L , the global matrix form of (2) is

$$\dot{\mathbf{z}}(t) = -L\mathbf{z}(t) + \mathbf{u}(t), \quad (3)$$

which implies that the agent state depends on the global input and the interaction between agents.

Discrete-time Observation Model: While the real dynamical model is continuous, the observed dynamics is discrete, and the observations are inevitably accompanied by noise. For sufficiently fast sampling, the agent state is piecewise stationary over time segments. One of the simplest method [24] to approximate (3) is

$$\tilde{\mathbf{z}}(k) = P\mathbf{z}(k-1) + \varepsilon\mathbf{u}(k-1) + \mathbf{e}_0(k), \quad (4)$$

where k indicates the discrete observation time, $\varepsilon > 0$ is the sampling period, which represents the weight of state discrepancy between time-adjacent observations, and $\mathbf{e}_0(k)$ is the observation noise, which satisfies independent and identical Gaussian distribution, i.e., $\mathbf{e}_0(k) \sim N(0, \sigma^2 I)$. The matrix $P = (I - \varepsilon L)$ is known as the interaction matrix, and it is readily seen that $P\mathbf{1} = \mathbf{1}$. To ensure that $\tilde{\mathbf{z}}(k)$ converges to the steady state asymptotically, we set $\varepsilon < 1/d_{\max}$ to have all the eigenvalues of P be within a unit circle [25], where d_{\max} is the maximum entry of D . Besides, define the vector set $\tilde{\mathcal{Z}} = \{\tilde{\mathbf{z}}(k) | k = 1, \dots, K\}$ as K time-series observations of a consensus process. Appropriate non-trivial information about P contained in $\tilde{\mathcal{Z}}$ is a necessary condition to infer the exact

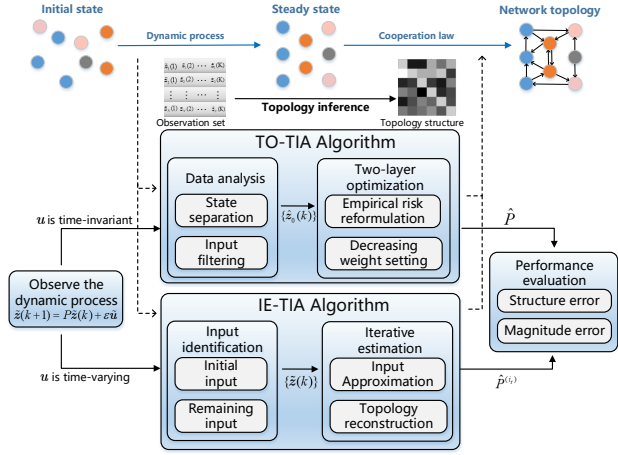


Fig. 1. An overview of TO-TIA and IE-TIA algorithms. First, TO-TIA or IE-TIA is selected according to the time-property. Then, we perform the selected algorithm using the given observations. Finally, the estimated P is obtained, and we analyze the performance of the proposed algorithms.

network topology [26]. Then, we have

$$\begin{aligned}\tilde{\mathbf{z}}(k+1) &= P(\tilde{\mathbf{z}}(k) - \mathbf{e}_0(k)) + \varepsilon \mathbf{u}(k) + \mathbf{e}_0(k+1) \\ &= P\tilde{\mathbf{z}}(k) + \varepsilon \mathbf{u}(k) + \mathbf{e}(k+1),\end{aligned}\quad (5)$$

where $\mathbf{e}(k+1) = \mathbf{e}_0(k+1) - P\mathbf{e}_0(k)$. Note that since (5) only illustrates the quantitative relationship between two consecutive observations, the observation noise will not affect the actual dynamics in the next moment.

B. Problem Description

Considering a network $\mathcal{G}(\mathcal{V}, \mathcal{E})$ where the agents satisfy the cooperation dynamics (3), the aim of this paper is to infer the underlying topology from observations. Note that (5) reflects the immediate interaction among connected agents by time-adjacent observations. Here, we adopt the empirical risk minimization model to characterize the interaction errors. Since real-world networks often exhibit specific characteristics, we introduce regularizers to fit the practical network property. Furthermore, the row stochastic property of interaction matrix is used as a constraint to guarantee the effectiveness of topology inference. Mathematically, we need to solve the following optimization problem,

$$\Phi_0 : \min_P \sum_{k=1}^{K-1} \|\tilde{\mathbf{z}}(k+1) - P\tilde{\mathbf{z}}(k) - \varepsilon \mathbf{u}(k)\|_2^2 + \rho \sum_{i=1}^N \|P_{[i]}\|_\ell \quad (6a)$$

$$\text{s.t. } P\mathbf{1} = \mathbf{1}, \quad (6b)$$

where the sum of $\|\cdot\|_2$ terms denotes the empirical risk, the ℓ -norm regularization term is characterized by the specified network property, and ρ is the non-negative regularization parameter. The constraint (6b) ensures the row stochasticity of the obtained P .

However, since the latent input is unmeasurable and no prior knowledge of it is available, Φ_0 is difficult to be solved directly. To tackle this issue, we propose TO-TIA and IE-TIA for different system dynamics, and the detailed conditions of them are formally stated as follows.

TO-TIA: the latent input is time-invariant and has already stimulated the network at the beginning of the observation.

IE-TIA: the latent input is time-varying and has not stimulated the network at the beginning of the observation.

It is worth remarking that TO-TIA is not a special case of IE-TIA. Furthermore, it provides direction for IE-TIA on how to identify the latent input and improve the inference accuracy, which will be discussed in detail in Section III and IV. An overview of the proposed algorithms is shown in Fig. 1.

IV. TO-TIA: DESIGN AND ANALYSIS

This section focuses on the time-invariant case. First, we analyze the separability of the coupled influence of initial system state and latent input, and provide an effective way to eliminate the influence of the input. Then, we propose a two-layer optimization strategy to improve the topology inference accuracy. Lastly, we provide detailed performance analysis for the proposed TO-TIA.

A. State Separation and Input Filtering

In this part, we perform state separation and filter out the influence of latent input from the global state. The analysis in this subsection also provides theoretical support for IE-TIA in Section IV. For ease of exposition, denote $\mathbf{u}(t)$ by \mathbf{u} . Lemma 1 describes the separability of the global state.

Lemma 1. *The global state $\mathbf{z}(t)$ is separable, and satisfies*

$$\mathbf{z}(t) = \mathbf{z}_0(t) + \mathbf{z}_u(t), \quad (7)$$

where

$$\begin{cases} \mathbf{z}_0(t) = \mathbf{v}_1 \mathbf{w}_1^T \mathbf{z}(0) + \sum_{i=2}^N e^{-\lambda_i t} \mathbf{v}_i \mathbf{w}_i^T \mathbf{z}(0), \\ \mathbf{z}_u(t) = \mathbf{v}_1 \mathbf{w}_1^T \mathbf{u} \cdot t + \mathbf{m} - \sum_{i=2}^N \frac{e^{-\lambda_i t}}{\lambda_i} \mathbf{v}_i \mathbf{w}_i^T \mathbf{u}, \end{cases} \quad (8)$$

$$\text{and } \mathbf{m} = \sum_{i=2}^N \frac{1}{\lambda_i} \mathbf{v}_i \mathbf{w}_i^T \mathbf{u}.$$

Lemma 1 illustrates that $\mathbf{z}(t)$ is separated into two parts: i) $\mathbf{z}_0(t)$ is generated by $\mathbf{z}(0)$, and converges asymptotically based on consensus protocol; ii) $\mathbf{z}_u(t)$ is generated by \mathbf{u} , and keeps updating for $t \geq 0$.

Clearly, $\mathbf{z}_0(t)$ is equivalent to the global state of a consensus process which is not influenced by external input, and satisfies $\dot{\mathbf{z}}_0(t) = -L\mathbf{z}_0(t)$. Thus, it applies well to solving Φ_0 by setting $\mathbf{u} = \mathbf{0}$. However, with unknown $\mathbf{z}(0)$ and \mathbf{u} , it is impossible to directly extract $\mathbf{z}_0(t)$ from $\mathbf{z}(t)$. To solve this problem, we first analyze the convergence of $\mathbf{z}(t)$. Unless otherwise noted, the continuous and discrete convergence time are referred as t_ϵ and k_ϵ throughout this paper, respectively. The time t_ϵ is given by

$$t_\epsilon = \inf\{t_0 : |\dot{z}_i(t) - \dot{z}_j(t)| < \epsilon, \forall i, j \in \mathcal{V}, \forall t > t_0\}. \quad (9)$$

Let $\mathbf{p}(k) = \tilde{\mathbf{z}}(k) - \tilde{\mathbf{z}}_N(k)\mathbf{1}$, then k_ϵ is obtained by

$$k_\epsilon = \inf\{k_0 : |p_i(k_0) - p_i(K)| < \epsilon\epsilon, \forall k_0 > 1, \forall i \in \mathcal{V}\}. \quad (10)$$

If $t \geq t_\epsilon$, the damping terms of $\mathbf{z}(t)$ decrease to zero, thus the state discrepancy in $\mathbf{z}_0(t)$ is negligible. It follows that

$$\mathbf{z}(t) = \mathbf{v}_1 \mathbf{w}_1^T \mathbf{u} \cdot t + \mathbf{v}_1 \mathbf{w}_1^T \mathbf{z}(0) + \mathbf{m}, \quad \forall t \geq t_\epsilon, \quad (11)$$

which describes the steady period of the dynamic process. Denote $\hat{\mathbf{z}}_0(t) = \mathbf{z}(t) - c\mathbf{1} \cdot t - \mathbf{r}$, and its discrete expression as $\hat{\mathbf{z}}_0(k)$. Then, we have the following theorem to further analyze the steady period.

Theorem 1. *Given arbitrary time-invariant \mathbf{u} , if $t \geq t_e$, then the global state satisfies*

$$\mathbf{z}(t) = c\mathbf{1} \cdot t + (I - \mathbf{v}_1 \mathbf{w}_1^T) \mathbf{r} + \mathbf{v}_1 \mathbf{w}_1^T \mathbf{z}(0), \quad (12)$$

where $c = \sum_{j=1}^N w_{1j} u_j$ and $\mathbf{r} = \mathbf{m} - m_N \mathbf{1}$. If $K \geq N + 1$, the estimation of P in the least square sense is optimal, given by

$$\hat{P} = \hat{Z}_0^{2:K} (\hat{Z}_0^{1:K-1})^T (\hat{Z}_0^{1:K-1} (\hat{Z}_0^{1:K-1})^T)^{-1}. \quad (13)$$

Remark 1. *Theorem 1 provides an effective way to eliminate the influence of \mathbf{u} from the global agent state, thereby revealing the feasibility of inferring network topology by solving Φ_0 .*

Equation (12) shows a new form of (11), where the global input is equivalent to $\mathbf{u} = c\mathbf{1} + L\mathbf{r}$. Define $\psi_0(t) = \|\mathbf{z}_0(t) - \hat{\mathbf{z}}_0(t)\|_2$ as the estimation error of $\mathbf{z}_0(t)$, and $\hat{\mathbf{z}}_0(k)$ as the discrete expression of $\hat{\mathbf{z}}_0(t)$. Theorem 2 analyzes the estimation error.

Theorem 2. *The estimation error of $\mathbf{z}_0(t)$ satisfies*

$$\psi_0(t) \leq e^{-\lambda_2 t} \|\mathbf{m}\|_2, \quad (14)$$

and decreases to zero exponentially, i.e.,

$$\lim_{t \rightarrow \infty} \psi_0(t) = 0. \quad (15)$$

Since λ_2 is the eigenvalue of Laplacian matrix, the estimation error is related to the network structure, which is unknown before we perform the topology inference. Nevertheless, Theorem 2 shows that $\psi_0(t)$ is bounded in a small range and only has a subtle impact on the initial converging period (See Appendix C for more details).

B. Two-Layer Optimization Strategy

To improve the inference accuracy using as few observations as possible, we reformulate Φ_0 from two aspects: empirical risk reformulation and the weight setting for the objective function. Then, a two-layer optimization strategy is designed to reduce the computation burden.

First, the higher-power property, $P^s = (P)^s$, is transformed into an additional empirical risk to the objective function (6a). Regardless of estimation error and observation noise, for $k + s \leq K$, we have

$$\hat{\mathbf{z}}_0(k + s) = P\hat{\mathbf{z}}_0(k + s - 1) = \dots = P^s \hat{\mathbf{z}}_0(k), \quad (16)$$

which reflects the constraint that P^s satisfies.

Second, different weight setting on the multiple terms of Φ_0 indicates a trade-off among different observations and yields different inference results. This inspires us to design an efficient weight setting to improve the inference accuracy further. To elaborate this effect, we consider three commonly used weight settings as follows. Given permutation $\{\alpha_1, \dots, \alpha_K\}$ satisfying $\sum_{i=1}^K \alpha_k = 1$, the decreasing (i.e., $\alpha_1 > \dots > \alpha_K$), increasing, and uniform weight setting are denoted by WS_1 ,

WS_2 , and WS_3 , respectively. On the one hand, the state discrepancy derived from the initial state decreases with k , indicating that smaller weight should be attached to $\hat{\mathbf{z}}_0(k)$ as k increases, i.e., using WS_1 . On the other hand, the estimation error of $\hat{\mathbf{z}}_0(k)$ decreases with k , indicating that larger weight should be attached to $\hat{\mathbf{z}}_0(k)$ as k increases, i.e., using WS_2 . WS_3 is adopted if there is no specific emphasis on different terms in Φ_0 , and is an intermediate setting for the comparison. Based on Theorem 2, we demonstrate that the topology inference result of Φ_0 is explicitly determined by the observations before the steady period, which plays a dominant role in the cooperation dynamics. Therefore, we adopt WS_1 to achieve the most accurate inference among the three settings, which will be verified by the simulation in Section V.

Combining the above two aspects, the initial optimization problem Φ_0 is reformulated as

$$\begin{aligned} \Phi_1 : \min_P \quad & \sum_{k=1}^{K-1} \alpha_k \|\hat{\mathbf{z}}_0(k+1) - P\hat{\mathbf{z}}_0(k)\|_2^2 + \rho \sum_{i=1}^N \|P_{[i]}\|_{\ell_1} \\ & + \beta \sum_{k=1}^{K-s} \sum_{s=1}^{K-N} \|\hat{\mathbf{z}}_0(k+s) - P^s \hat{\mathbf{z}}_0(k)\|_2^2 \end{aligned} \quad (17a)$$

$$\text{s.t. (6b) and } \text{WS}_1 \text{ for } \alpha_k \text{ hold,} \quad (17b)$$

where ℓ_1 -norm is adopted to promote the sparsity of network [27], [28], ρ is a non-negative regularization parameter, and $\beta \in (0, 1]$ is the parameter to balance the terms of the objective function. To reduce the computation burden, we further decouple Φ_1 into a two-layer optimization problem to avoid directly solving the s -power equations about the entries in P . First, we turn to directly obtain all P^s by solving the first layer sub-problem

$$\Phi_{1_a} : \min_{P^s} \sum_{k=1}^{K-s} \|\hat{\mathbf{z}}_0(k+s) - P^s \hat{\mathbf{z}}_0(k)\|_2^2 \quad (18a)$$

$$\text{s.t. (6b) holds.} \quad (18b)$$

By solving Φ_{1_a} for $s = 1, \dots, K - N$, the set $\mathcal{P}^s = \{\hat{P}^s\}$ is obtained. Then, we have the second layer sub-problem

$$\begin{aligned} \Phi_{1_b} : \min_P \quad & \sum_{k=1}^{K-1} \alpha_k \|\hat{\mathbf{z}}_0(k+1) - P\hat{\mathbf{z}}_0(k)\|_2^2 + \rho \sum_{i=1}^N \|P_{[i]}\|_{\ell_1} \\ & + \beta \sum_{s=1}^{K-N} \|(\hat{P}^s - P\hat{P}^{s-1})\|_F^2 \end{aligned} \quad (19a)$$

$$\text{s.t. (6b) and } \text{WS}_1 \text{ for } \alpha_k \text{ hold,} \quad (19b)$$

where $\|\cdot\|_F$ denotes the Frobenius norm of a matrix. Note that optimization problem Φ_{1_a} and Φ_{1_b} are convex, and many efficient methods are suitable to solve them, e.g., ADMM [20], [29] and truncated Newton interior-point method [30]. By solving Φ_{1_b} , the final estimation \hat{P} is obtained.

C. Description of TO-TIA and Performance Evaluation

Based on the previous discussion, the topology inference algorithm for the time-invariant input is summarized as TO-TIA. It first eliminates the influence of \mathbf{u} to estimate $\hat{\mathbf{z}}_0(k)$, then performs the two-layer optimization strategy to obtain the estimated P . The details are shown in Algorithm 1.

Algorithm 1: TO-TIA

Input: Observation set $\tilde{\mathcal{Z}}$, sampling period ε **Output:** Estimated interaction matrix \hat{P} 1: $K = |\tilde{\mathcal{Z}}|$;2: Calculate k_ε by (10);3: $c\mathbf{1} = \frac{1}{K-k_\varepsilon} \sum_{k=k_\varepsilon}^{K-1} \frac{\tilde{\mathbf{z}}(k+1) - \tilde{\mathbf{z}}(k)}{\varepsilon}$;4: $\mathbf{r} = \frac{1}{K-k_\varepsilon+1} \sum_{k=k_\varepsilon}^K (\tilde{\mathbf{z}}(k) - \tilde{z}_N(k)\mathbf{1})$;5: $\hat{\mathbf{z}}_0(k) = \tilde{\mathbf{z}}(k) - c\mathbf{1} \cdot k - \mathbf{r}$;6: **for** $s \leftarrow 1$ **to** $K - N$ **do**7: Obtain \hat{P}^s by solving Φ_{1_a} using $\{\hat{\mathbf{z}}_0(k)\}$;8: **end for**9: Obtain \hat{P} by solving Φ_{1_b} using $\{\hat{P}^s\}$.TABLE II
ALGORITHM DESCRIPTION

Algorithm	Parameter setting	Estimation error
A ₁	$\beta = 0$	ψ_m^1
A ₂	WS ₂ for α_k holds	ψ_s^2, ψ_m^2
A ₃	WS ₃ for α_k holds	ψ_s^3, ψ_m^3

Two evaluation criteria are designed to describe the inference result sufficiently. First, define ψ_s as the structure error to reflect the network structure, given by

$$\psi_s = \frac{\sum_{i=1}^N \sum_{j=1}^N \text{sign}(\hat{P}_{ij} - P_{ij})}{N^2}, \quad (20)$$

where $\text{sign}(\cdot)$ is an indicative function, which is set to 1 if (\cdot) is non-zero, and 0 otherwise. Second, define ψ_m as the magnitude error to reflect the network edge weight, given by

$$\psi_m = \frac{\|\hat{P} - P\|_F^2}{\|P\|_F^2}. \quad (21)$$

By the above definition, let ψ_s^* and ψ_m^* be the structure error and magnitude error of the estimated P obtained by TO-TIA, respectively. We compare TO-TIA with three conventional algorithms, and the difference between them and TO-TIA are shown in TABLE II. Comparing with IF-TIA, A₁ lacks the empirical risk reformulation, A₂ adopts the increasing weight setting, and A₃ adopts the uniform weight setting for the objective function. Theorem 3 summarizes the comparative results of these algorithms.

Theorem 3. (Performance of TO-TIA) *Given noisy observation set, the followings are true:*

i) Comparing with A₁, the empirical risk reformulation in TO-TIA decreases the magnitude error, i.e., $\psi_m^* < \psi_m^1$;

ii) Comparing with A₂ and A₃, the decreasing weight setting in TO-TIA decreases both the structure and magnitude errors, i.e., $\psi_s^* < \psi_s^2 < \psi_s^3$, $\psi_m^* < \psi_m^2 < \psi_m^3$.

Theorem 3 reveals that the two-layer optimization strategy yields higher inference accuracy than the conventional optimization strategies.

V. IE-TIA: DESIGN AND ANALYSIS

In this section, we first analyze the identifiability of the time-varying input. Then, an iterative estimation strategy is proposed to improve the accuracy of the estimated network topology and time-varying input. Lastly, we summarize the proposed algorithm as IE-TIA and provide detailed theoretical analysis to show its performance.

A. Input Identification

In this part, we analyze the identifiability of time-varying input. By Lemma 1, we observe that the first term of $\mathbf{z}_0(t)$ in (8) is a vector in which all entries are the same constant, and the entry of the second term of $\mathbf{z}_0(t)$ is essentially a linear superposition of $e^{-\lambda_i t}$. Hence, the entry of $\mathbf{z}_0(t)$ is Lipschitz continuous on t , and satisfies

$$|z_{0_j}(t_2) - z_{0_j}(t_1)| \leq l_j |t_2 - t_1|, \forall t_1, t_2 > 0, \quad (22)$$

where l_j is called the Lipschitz constant of agent j . Let l be the maximum Lipschitz constant, given by

$$l = \max \{l_j, j \in \mathcal{V}\}. \quad (23)$$

Note that if the latent input is sufficiently small, it has no ability to alter the information transmitted by the injected agent. To avoid this meaningless situation, Definition 1 describes the condition of the identifiable case we will focus on.

Definition 1. *The latent input is said to be identifiable if*

$$\left| \frac{z_j(t + \Delta t) - z_j(t)}{u_j(t)\Delta t} \right| < l, \quad (24)$$

where $\Delta t > 0$ is arbitrarily small.

In the discrete-time observation model, define k_{u_j} as the injection time when latent input begins to affect the network via agent j , i.e., $u_j(k) = 0$ for $k < k_{u_j}$, and remodel (5) as

$$\tilde{\mathbf{z}}_j(k+1) = \begin{cases} P_{[j]} \tilde{\mathbf{z}}(k) + e_j(k+1), & \text{if } k < k_{u_j}, \\ P_{[j]} \tilde{\mathbf{z}}(k) + \varepsilon u_j(k) + e_j(k+1), & \text{if } k \geq k_{u_j}. \end{cases} \quad (25)$$

Suppose that the latent input is injected into the network via agent q initially. As a result of the network diffusion, once agent q is injected by latent input, the global dynamics will be influenced. Define the function $h_1(j, k)$, given by

$$h_1(j, k) = \left| \frac{\tilde{z}_j(k) - \tilde{z}_j(k-1)}{\tilde{z}_j(k-1) - \tilde{z}_j(k-2)} \right| - \frac{1}{l} - 1. \quad (26)$$

Then, Proposition 1 states how to identify q and k_{u_q} .

Proposition 1. *If the latent input satisfies (24), then k_{u_q} and q are respectively identified by*

$$\begin{aligned} k_{u_q} &= \inf \{k_0 : h_1(i, k_0) < 0, h_1(i, k_0 + 1) \geq 0, \\ &\quad \forall i \in \mathcal{V}, \forall k_0 > 1\}, \\ q &= \inf \{i : h_1(i, k_{u_q}) < 0, h_1(i, k_{u_q} + 1) \geq 0, \forall i \in \mathcal{V}\}. \end{aligned} \quad (27)$$

Note that if more than one agent is injected at time k_{u_q} , the agent with the minimum agent number is selected as the initially injected agent.

Remark 2. By Proposition 1, the time-invariant/varying property of latent input is identified, thereby the corresponding inference algorithm is determined. If (27) has no solution, then the latent input is time-invariant, and the inference problem should be solved by TO-TIA proposed in Section III.

Define $\mathbf{z}_\varphi(k)$ as the data in which the latent input at time $k-1$ is filtered, given by $\mathbf{z}_\varphi(k) = \tilde{\mathbf{z}}(k) - \varepsilon\mathbf{u}(k-1)$. Then, the observation model (5) is rewritten as

$$\tilde{\mathbf{z}}(k) = \begin{cases} \mathbf{z}_\varphi(k), & \text{if } k \leq k_{u_q}, \\ \mathbf{z}_\varphi(k) + \varepsilon\mathbf{u}(k-1), & \text{if } k > k_{u_q}, \end{cases} \quad (29)$$

and $\tilde{\mathcal{Z}}$ is divided into two subsets, given by

$$\tilde{\mathcal{Z}} = \underbrace{\{\tilde{\mathbf{z}}(1), \dots, \tilde{\mathbf{z}}(k_{u_q})\}}_{\text{subset } \tilde{\mathcal{Z}}_1} \cup \underbrace{\{\tilde{\mathbf{z}}(k_{u_q}+1), \dots, \tilde{\mathbf{z}}(K)\}}_{\text{subset } \tilde{\mathcal{Z}}_2}, \quad (30)$$

where $\tilde{\mathcal{Z}}_1$ consists of the observations that are not affected by latent input, and $\tilde{\mathcal{Z}}_2$ consists of the remaining observations that are affected by latent input. Since $\tilde{\mathcal{Z}}_1$ reflects the interactions between agents directly, it applies well to obtain an initially estimated P , denoted by $\hat{P}^{(0)}$. However, if $k_{u_q} < N+1$, then Φ_{1_a} becomes infeasible and $\mathcal{P}^s = \emptyset$. In this case, we reformulate Φ_1 as Φ_2 , in which only the decreasing weight setting is adopted to improve the inference accuracy, given by

$$\Phi_2 : \min_P \sum_{k=1}^{k_{u_q}-1} \alpha_k \|\tilde{\mathbf{z}}(k+1) - P\tilde{\mathbf{z}}(k)\|_2^2 + \rho \sum_{i=1}^N \|P_{[i]}\|_{\ell_1} \quad (31a)$$

$$\text{s.t. (6b) and WS}_1 \text{ for } \alpha_k \text{ hold.} \quad (31b)$$

Define \mathcal{V}_u as the agent set, which consists of all the injected agents, and similar to $h_1(j, k)$, define $h_2(j, k)$ as the function to identify all the remaining injected agents, given by

$$h_2(j, k) = \left| \frac{\hat{P}_{[j]}^{(0)} \tilde{\mathbf{z}}(k-1) - \tilde{z}_j(k-1)}{\tilde{z}_j(k) - \hat{P}_{[j]}^{(0)} \tilde{\mathbf{z}}(k-1)} \right| - l. \quad (32)$$

Then, Proposition 2 states how to obtain \mathcal{V}_u .

Proposition 2. If $j \in \mathcal{V}_u \setminus \{q\}$, then

$$k_{u_j} = \inf\{k_0 : h_2(j, k) > 0, h_2(j, k+1) \leq 0, \forall k_0 \geq k_{u_q}\}. \quad (33)$$

Proposition 1 and 2 show the identifiability of all the injected agents and injection time, and provide theoretical support to estimate the latent input in the following subsection. Furthermore, they provide an alternative, efficient, and computationally reliable way of monitoring, detecting, and pinpointing the real-time faults of cooperation dynamics, thereby avoiding the catastrophic failures in practical scenarios.

B. Iterative Estimation Strategy

By the previous subsection, the set $\tilde{\mathcal{Z}}_1$ is utilized to estimate P . However, since $\tilde{\mathcal{Z}}_1$ cannot cover the information of the whole dynamic process, it is not sufficient to obtain an accurate inference result. To make full use of the valuable information of all the observations in $\tilde{\mathcal{Z}}$, an iterative estimation strategy is proposed. Define $\hat{u}_j^{(i)}(k)$ and $\hat{P}^{(i)}$ as the estimation of $u_j(k)$

and P at the i -th iteration, respectively, and the iteration is separated into the following four steps.

The first step is to estimate $\mathbf{u}(k)$. Considering a one-step prediction of $\tilde{\mathbf{z}}(k-1)$, we have

$$\tilde{z}_j(k) = P_{[j]} \tilde{\mathbf{z}}(k-1) + \varepsilon u_j(k-1). \quad (34)$$

Accordingly, at the i -th iteration, the estimation of $u_j(k)$ is

$$\hat{u}_j^{(i)}(k) = \begin{cases} 0, & \text{if } k < k_{u_j}, \\ \frac{1}{\varepsilon}(\tilde{z}_j(k) - \hat{P}_{[j]}^{(i-1)} \tilde{\mathbf{z}}(k-1)), & \text{if } k \geq k_{u_j}. \end{cases} \quad (35)$$

The second step is to approximate the expression of $\mathbf{u}(k)$. Define $u_j^{(i)}(k; \boldsymbol{\theta}_j)$ as the functional form of $\hat{u}_j^{(i)}(k)$, where $\boldsymbol{\theta}_j$ represents the coefficient vector (e.g., if $u_j^{(i)}(k; \boldsymbol{\theta}_j) = ak^2 + bk + c$, then $\boldsymbol{\theta}_j = [a, b, c]^T$). Many estimation algorithms (e.g., the least square estimate [31]) are computationally efficient to calculate $\boldsymbol{\theta}_j$ by solving

$$\hat{\boldsymbol{\theta}}_j = \arg \min_{\boldsymbol{\theta}_j} \sum_{k=1}^K (u_j^{(i)}(k; \boldsymbol{\theta}_j) - \hat{u}_j^{(i)}(k))^2. \quad (36)$$

The third step is to reconstruct P . Different from obtaining $\hat{P}^{(0)}$ using $\tilde{\mathcal{Z}}_1$, $\tilde{\mathcal{Z}}_2$ is also used to estimate P during the iteration. At the i -th iteration, $z_{\varphi_j}(k)$ is estimated by

$$\hat{z}_{\varphi_j}^{(i)}(k) = \begin{cases} \tilde{z}_j(k), & \text{if } k \leq k_{u_j}, \\ \tilde{z}_j(k) - \varepsilon \hat{u}_j^{(i)}(k_{u_j}; \hat{\boldsymbol{\theta}}_j), & \text{if } k = k_{u_j} + 1, \\ \hat{P}_{[j]}^{(i-1)} \hat{\mathbf{z}}_{\varphi}^{(i)}(k-1), & \text{if } k > k_{u_j} + 1. \end{cases} \quad (37)$$

Then, by solving Φ_1 using $\{\hat{\mathbf{z}}_{\varphi}^{(i)}(k)\}$, $\hat{P}^{(i)}$ is obtained.

The fourth step is to determine whether to terminate the iteration. Define $\psi_d^{(i)}$ as the magnitude difference between $\hat{P}^{(i)}$ and $\hat{P}^{(i-1)}$, given by

$$\psi_d^{(i)} = \frac{\|\hat{P}^{(i)} - \hat{P}^{(i-1)}\|_F^2}{\|\hat{P}^{(i-1)}\|_F^2}. \quad (38)$$

The iteration is terminated if

$$\psi_d^{(i)} < \delta_d, \quad (39)$$

where $\delta_d > 0$ is a positive termination tolerance. Suppose the algorithm terminates at the i_t -th iteration, the final estimation is $\hat{P}^{(i_t)}$.

Remark 3. The key insight of the whole iteration process is to alternately optimize the network topology and the coefficients of the latent input, which ensures that the iteration returns the most suitable topology for the noisy observations.

C. Description of IE-TIA and Performance Evaluation

Based on the previous discussion, the topology inference algorithm for the time-varying input is summarized as IE-TIA, which consists of three stages: i) identify the agent that is initially injected by latent input, ii) identify the remaining agents that are injected by latent input subsequently, and iii) perform the iteration to estimate the latent input and network topology. The details are shown in Algorithm 2.

IE-TIA is feasible for many practical applications, e.g., monitor cascading failures in power grids, capture the interaction relationship in social networks, and predict the movement

Algorithm 2: IE-TIA

Input: Observation set $\tilde{\mathcal{Z}}$, iteration threshold δ_d
Output: Estimated interaction matrix $\hat{P}^{(i_t)}$

- 1: **Initialize:** Iteration step $i = 1$, iteration error $\hat{\psi}_m^{(1)} \leftarrow \delta_d$;
- 2: Calculate k_{u_q} by (27);
- 3: Calculate q by (28);
- 4: **if** $k_{u_q} \leq N$ **then**
- 5: Obtain $\hat{P}^{(0)}$ by solving Φ_2 ;
- 6: **else**
- 7: Obtain $\hat{P}^{(0)}$ by solving Φ_1 ;
- 8: **end if**
- 9: Obtain \mathcal{V}_u by Proposition 2;
- 10: **while** $\psi_d^{(i)} \geq \delta_d$ **do**
- 11: **for** $j \in \mathcal{V}$ **do**
- 12: **for** $k = 1 : K$ **do**
- 13: **if** $j \in \mathcal{V}_u$ **then**
- 14: Calculate $\hat{u}_j^{(i)}(k)$, $\hat{\theta}_j^{(i)}$, $\hat{z}_{\varphi_j}^{(i)}(k)$ by (35), (36), (37);
- 15: **else**
- 16: Set $\hat{u}_j^{(i)}(k) = 0$, $\hat{\theta}_j^{(i)} = \mathbf{0}$, and $\hat{z}_{\varphi_j}^{(i)}(k) \leftarrow \tilde{z}_j(k)$;
- 17: **end if**
- 18: **end for**
- 19: **end for**
- 20: Obtain $\hat{P}^{(i)}$ by solving Φ_1 using $\{\hat{\mathbf{z}}_\varphi^{(i)}\}$;
- 21: Calculate $\psi_d^{(i)}$ by (38) ;
- 22: $i = i + 1$;
- 23: **end while**
- 24: $i_t \leftarrow i$;
- 25: Obtain the final estimation $\hat{P}^{(i_t)}$.

of birds flocking. To evaluate the performance of the iterative estimation strategy in IE-TIA, we have the following definition. We adopt a quadratic error criterion [32] to evaluate whether the real $u_j^{(i)}(k)$ is well estimated by $\hat{u}_j^{(i)}(k; \hat{\theta}_j)$ on the injection interval $[k_{u_j}, K]$ and the interval before k_{u_j} , i.e.,

$$\psi_\theta^{(i)} = \frac{1}{KN} \sum_{j=1}^N \sum_{k=1}^K \|u_j(k) - \hat{u}_j^{(i)}(k; \hat{\theta}_j)\|_2^2. \quad (40)$$

Note that $\psi_\theta^{(i)}$ also reflects the performance of Proposition 1 and Proposition 2, in terms of the utilization of the data before time k_{u_j} . Besides, define $\psi_m^{(i)}$ as the magnitude error of $\hat{P}^{(i)}$, given by

$$\psi_m^{(i)} = \frac{\|P - \hat{P}^{(i)}\|_F^2}{\|P\|_F^2}. \quad (41)$$

Define P^* as the optimal estimation of P in the least square sense, and by the definition of $\mathbf{z}_\varphi(k)$, it is expressed as

$$P^* = Z_\varphi^{2:K} (Z_\varphi^{1:K-1})^T (Z_\varphi^{1:K-1} (Z_\varphi^{1:K-1})^T)^{-1}. \quad (42)$$

Theorem 4. (Performance of IE-TIA) Given noisy observation set, the followings are true:

i) IE-TIA decreases the estimation error with the iteration continuously, i.e.,

$$\begin{cases} \psi_\theta^{(i_t)} < \dots < \psi_\theta^{(2)} < \psi_\theta^{(1)}, \\ \psi_m^{(i_t)} < \dots < \psi_m^{(2)} < \psi_m^{(1)}; \end{cases} \quad (43)$$

ii) The algorithm complexity of IE-TIA is $O(\frac{\psi_m^{(0)}}{\delta_m})$;

iii) If $k_{u_q} \geq N + 1$, then

$$\lim_{i \rightarrow \infty} \hat{P}^{(i)} = P^*. \quad (44)$$

Theorem 4 provides a compelling result that the iterative estimation strategy asymptotically approaches the optimal estimation in the least square sense, and the convergence of IE-TIA is guaranteed.

Remark 4. While the latent input is unknown in practice, the iterative estimation strategy gives guarantees on its estimation accuracy, which in turn implies guarantees on the accuracy of the inferred network topology.

We consider a special dynamic process by defining a new variable $\mathbf{u}(y(t), n) = [0, \dots, y(t), \dots, 0]^T$, where $y(t)$ is the n -th entry of $\mathbf{u}(y(t), n)$. N independent inference results are obtained by using N different dynamic processes, which are generated by setting $\mathbf{u}(t) = \mathbf{u}(y(t), n)$ for $n \in \mathcal{N}$. Define $\psi_m(n)$ as the magnitude error of the estimated P , which is obtained by using the observations of the n -th dynamic process, and define $\Psi = \{\psi_m(n), n \in \mathcal{N}\}$ as the set of magnitude error. The following corollary provides a permutation of $\psi_m(n)$.

Corollary 1. Given $\mathcal{G}(\mathcal{V}, \mathcal{E})$, stimulating different agent with the same input yields different inference accuracy, i.e.,

$$\sigma_1(\Psi) \geq \sigma_2(\Psi) \geq \dots \geq \sigma_N(\Psi), \quad (45)$$

where $\sigma_1(\Psi) = \max\{\Psi\}$ and $\sigma_N(\Psi) = \min\{\Psi\}$.

The key point to get Corollary 1 is that stimulating different agent yields different interaction among agents. Specifically, (45) takes the equal sign when the network is composed of a complete graph. Corollary 1 shows the feasibility of improving the inference accuracy by stimulating particular agents if the input is controllable.

VI. SIMULATION

In this section, we conduct extensive simulations to demonstrate the performance of TO-TIA and IE-TIA in terms of the estimation error for different directed networks, and illustrate the corresponding theoretical results. Without loss of generality, all networks and initial system states are randomly generated with the connectivity guaranteed, and each simulation is conducted by the observations of a single dynamic process.

A. Performance of TO-TIA

In this part, the simulations are divided into two parts to illustrate the effectiveness of the two-layer optimization strategy in TO-TIA, and validate the conclusions of Theorem 3. The simulation results are shown in Fig. 2 and Fig. 3.

First, to validate the empirical risk reformulation, we compare the magnitude error of the estimated P obtained by TO-TIA and A_1 . The line with diamond (square) markers corresponds to the error of TO-TIA (A_1). Fig. 2(a) shows the relationship between the magnitude error and the variance of the observation noise σ^2 , where the network consists of 10 nodes and $\sigma^2 \in \{0.1, 0.2, \dots, 1\}$. Fig. 2(b) shows the relationship between the magnitude error and network size N , where $N \in \{5, 10, \dots, 30\}$ and $\sigma^2 = 0.3$. Fig. 2 shows that as σ^2 or N increases, the error of TO-TIA keeps being the

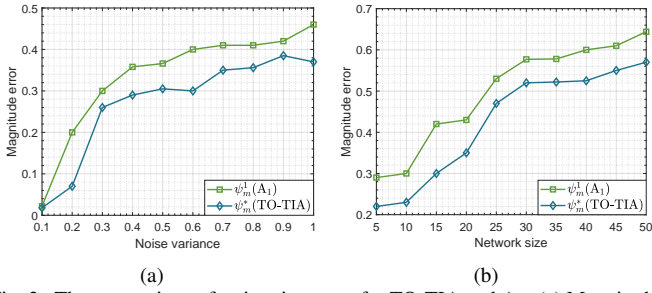


Fig. 2. The comparison of estimation error for TO-TIA and A_1 . (a) Magnitude error with different noise variance. (b) Magnitude error with different network size.

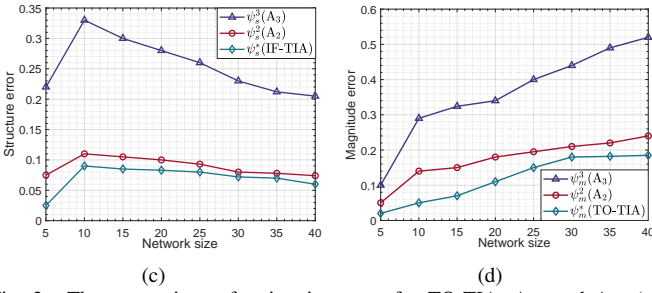
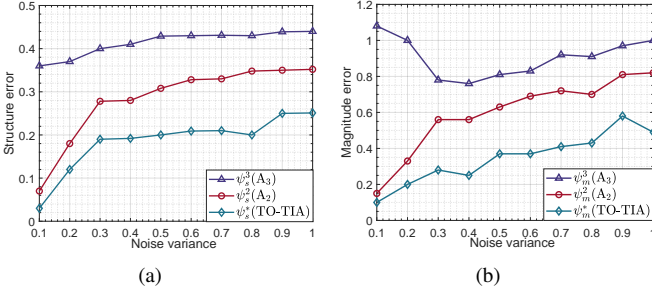


Fig. 3. The comparison of estimation error for TO-TIA, A_2 , and A_3 . (a) Structure error with different noise variance. (b) Magnitude error with different noise variance. (c) Structure error with different network size. (d) Magnitude error with different network size.

smallest, i.e., $\psi_m^* < \psi_m^1$. Therefore, the reformulated empirical risk improves the inference accuracy.

Second, to validate the decreasing weight setting, we compare the magnitude errors and structure errors of the estimated P obtained by TO-TIA, A_2 , and A_3 . The line with diamond(triangle or circle) markers corresponds to the error of TO-TIA (A_2 or A_3). Fig. 3(a) and Fig. 3(b) show the relationships between the estimation error and the variance of the observation noise σ^2 , where the network consists of 12 nodes and $\sigma^2 \in \{0.1, 0.2, \dots, 1\}$. Fig. 3(c) and Fig. 3(d) show the relationships between the estimation error and network size N , where $N \in \{5, 10, \dots, 40\}$ and $\sigma^2 = 0.2$. Fig. 3 shows that as σ^2 or N increases, the error of TO-TIA keeps being the smallest, and the error of A_3 keeps being the largest, i.e., $\psi_s^* < \psi_s^2 < \psi_s^3$ and $\psi_m^* < \psi_m^2 < \psi_m^3$. Therefore, both structure error and magnitude error are decreased by the decreasing weight setting.

B. Performance of IE-TIA

In this part, the simulations are divided into two parts to illustrate the effectiveness of IE-TIA. Analogous to $\psi_\theta^{(i)}$, define

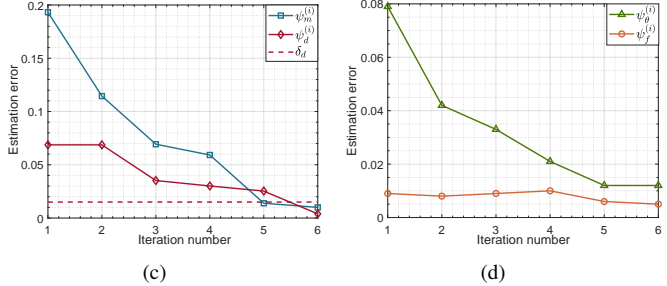
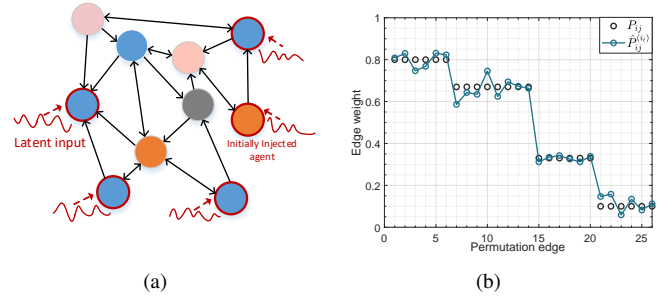


Fig. 4. Iterative performance of IE-TIA. (a) A visual representation of the network. (b) Off-diagonal entries of P and $\hat{P}^{(i_t)}$. (c) Estimation error of P during the iteration. (d) Estimation error of $\mathbf{u}(k)$ during the iteration.

$\psi_f^{(i)}$ as the fitting error to evaluate whether $\hat{u}_j^{(i)}(k)$ is well fitted by $\hat{u}_j^{(i)}(k; \hat{\theta}_j)$, given by

$$\psi_f^{(i)} = \frac{1}{KN} \sum_{j=1}^N \sum_{k=1}^K \|\hat{u}_j^{(i)}(k) - \hat{u}_j^{(i)}(k; \hat{\theta}_j)\|_2^2. \quad (46)$$

The functional form of the input is $u_i(k; \theta_i) = ae^{-bk} + c$, where θ_i is generated under the constraint (24), and all injected nodes and injection time are selected randomly. The simulation results are shown in Fig. 4 and TABLE III.

First, to illustrate the performance of the iterative estimation strategy in IE-TIA, we numerically simulate the randomly generated network with $N = 10$ nodes. The detailed description of the network is demonstrated by Fig. 4(a). In Fig. 4(b), we display the off-diagonal entries of the true interaction matrix P and the estimated P with discrete dots and the dots connected by a line, respectively, and all entries are sorted by value. Fig. 4(c) shows the estimation error of P in the iteration process. The line with diamond markers corresponds to the estimation error at each iteration, the line with cross markers corresponds to the magnitude difference between two adjacent iterations, and the dashed line represents the termination tolerance. As shown in Fig. 4(c), both the estimation error $\psi_m^{(i)}$ and the iteration difference $\psi_d^{(i)}$ keep decreasing. The stopping condition (39) will be satisfied gradually, and is met at the 6-th iteration ($\psi_d^{(6)} < \delta_d$). Fig. 4(d) shows the estimation and fitting error of $\mathbf{u}(k)$ in the iteration process. The line with square (triangle) markers corresponds to the estimation (fitting) error of $\mathbf{u}(k)$. It shows that $\psi_\theta^{(i)}$ keeps decreasing and $\psi_f^{(i)}$ keeps small. By Fig. 4(c) and 4(d), we have $\psi_\theta^{(6)} < \dots < \psi_\theta^{(1)}$ and $\psi_m^{(6)} < \dots < \psi_m^{(1)}$, which validates the first conclusion of Theorem 4.

Second, we illustrate the effectiveness and algorithm complexity of IE-TIA. The probability of each node being in-

TABLE III
THE SIMULATION RESULTS OF IE-TIA

Size N	10	20	30	40	50	60
Iteration i_t	5	6	5	6	7	5
Error $\psi_m^{(i_t)}$	0.189	0.236	0.360	0.341	0.525	0.533

jected by input is 0.5, and we set the termination tolerance $\delta_d = 0.015$ for all simulations. TABLE III lists the iteration number and estimation error with different network size. It shows that as the network size increases, IE-TIA terminates with stable algorithm complexity.

VII. CONCLUSION

In this paper, we proposed TO-TIA and IE-TIA to learn the directed network topology from the observations of cooperation dynamics, where the latent input injected into the network is unmeasurable. We first proposed TO-TIA towards the time-invariant input: i) an input filtering method was designed to eliminate the influence of latent input on the dynamic process, and ii) a two-layer optimization strategy was proposed to improve the topology inference accuracy. We then proposed IE-TIA towards the time-varying input: i) an identification method was designed to identify all the injected agents, and ii) an iterative estimation strategy was proposed to improve the accuracy of the estimation of the network topology and latent input. Furthermore, we provided strict theoretical analysis and comprehensive simulations to illustrate the effectiveness and the accuracy of TO-TIA and IE-TIA.

One of the promising future directions of this work is to utilize the latent input to steer the network to a target state. The potential challenges mainly lie in how to select the injected agents and guarantee the controllability of the dynamical system. We believe that by paying off efforts, new favorable alternatives will be provided for multi-agent cooperative control.

APPENDIX

A. Proof of Lemma 1

Proof. We first write the agent state in the model decomposition form. The integral form of (3) is given by

$$\mathbf{z}(t) = e^{-Lt}\mathbf{z}(0) + \int_0^t e^{-L(t-\tau)}\mathbf{u}d\tau. \quad (47)$$

By combining $L = MJM^{-1}$, we have

$$\begin{aligned} e^{-Lt} &= e^{-MJM^{-1}t} \\ &= M \begin{bmatrix} e^0 & 0 & \cdots & 0 \\ 0 & e^{-\lambda_2 Jt} & \cdots & 0 \\ \vdots & \vdots & \ddots & \vdots \\ 0 & 0 & 0 & e^{-\lambda_N Jt} \end{bmatrix} M^{-1} \\ &= \sum_{i=1}^N e^{-\lambda_i t} \mathbf{v}_i \mathbf{w}_i^T. \end{aligned} \quad (48)$$

It follows that the first term of (47) is rewritten as

$$\begin{aligned} \mathbf{z}_0(t) &= e^{-Lt}\mathbf{z}(0) = \sum_{i=1}^N e^{-\lambda_i t} \mathbf{v}_i \mathbf{w}_i^T \mathbf{z}(0) \\ &= \mathbf{v}_1 \mathbf{w}_1^T \mathbf{z}(0) + \sum_{i=2}^N e^{-\lambda_i t} \mathbf{v}_i \mathbf{w}_i^T \mathbf{z}(0), \end{aligned} \quad (49)$$

and is generated by $\mathbf{z}(0)$. The second term of (47) satisfies

$$\begin{aligned} \mathbf{z}_u(t) &= \int_0^t e^{-L(t-\tau)}\mathbf{u}d\tau = \int_0^t \sum_{i=1}^N e^{-\lambda_i(t-\tau)} d\tau \cdot \mathbf{v}_i \mathbf{w}_i^T \mathbf{u} \\ &= \mathbf{v}_1 \mathbf{w}_1^T \mathbf{u} \cdot t + \sum_{i=2}^N \frac{1}{\lambda_i} \mathbf{v}_i \mathbf{w}_i^T \mathbf{u} - \sum_{i=2}^N \frac{e^{-\lambda_i t}}{\lambda_i} \mathbf{v}_i \mathbf{w}_i^T \mathbf{u}, \end{aligned} \quad (50)$$

and is generated by \mathbf{u} . This concludes the proof. \square

B. Proof of Theorem 1

Proof. We first proof (12) by inducing two facts, i.e.,

$$\mathbf{v}_1 = \mathbf{1}, \quad \mathbf{w}_i^T \mathbf{v}_j = 0 \quad (i \neq j). \quad (51)$$

It follows that the first term of (11) satisfies

$$\mathbf{v}_1 \mathbf{w}_1^T \mathbf{u} \cdot t = \sum_{j=1}^N w_{1j} u_j \mathbf{1} \cdot t = c \mathbf{1} \cdot t, \quad (52)$$

where $c = \sum_{j=1}^N w_{1j} u_j$. Setting $\mathbf{u}_1 = c \mathbf{1}$ and taking it into the third term of (11), we have

$$\sum_{i=2}^N \frac{1}{\lambda_i} \mathbf{v}_i \mathbf{w}_i^T \mathbf{u}_1 = c \sum_{i=2}^N \frac{1}{\lambda_i} \mathbf{v}_i \mathbf{w}_i^T \mathbf{v}_1 = \mathbf{0}. \quad (53)$$

Setting $\mathbf{u}_2 = L\mathbf{r}$, where \mathbf{r} is a non-zero vector, and taking it into the first term of (11), we have

$$\begin{aligned} \mathbf{v}_1 \mathbf{w}_1^T \mathbf{u}_2 \cdot t &= \mathbf{v}_1 \mathbf{w}_1^T L\mathbf{r} \cdot t \\ &= \left(\sum_{i=2}^N \mathbf{v}_i \mathbf{w}_1^T \mathbf{v}_i \mathbf{w}_i^T \lambda_i \right) \mathbf{r} \cdot t \\ &= \mathbf{0}. \end{aligned} \quad (54)$$

Similarly, taking \mathbf{u}_2 into the third term of (11), we have

$$\begin{aligned} \sum_{i=2}^N \frac{1}{\lambda_i} \mathbf{v}_i \mathbf{w}_i^T \mathbf{u}_2 &= \sum_{i=2}^N \frac{1}{\lambda_i} \mathbf{v}_i \mathbf{w}_i^T L\mathbf{r} \\ &= \sum_{i=2}^N \frac{1}{\lambda_i} \mathbf{v}_i \mathbf{w}_i^T \left(\sum_{i=1}^N \mathbf{v}_i \mathbf{w}_i^T \lambda_i \right) \mathbf{r} \\ &= \sum_{i=2}^N \mathbf{v}_i \mathbf{w}_i^T \mathbf{r} \\ &= (I - \mathbf{v}_1 \mathbf{w}_1^T) \mathbf{r}. \end{aligned} \quad (55)$$

The square matrix $(I - \mathbf{v}_1 \mathbf{w}_1^T)$ satisfies

$$\det(I - \mathbf{v}_1 \mathbf{w}_1^T) = \begin{vmatrix} 1 - w_{11} & -w_{12} & \cdots & -w_{1N} \\ -w_{11} & 1 - w_{12} & \cdots & -w_{1N} \\ \vdots & \vdots & \ddots & \vdots \\ -w_{11} & -w_{12} & \cdots & 1 - w_{1N} \end{vmatrix}$$

$$= (1 - \sum_{i=1}^N w_{1i}) \begin{vmatrix} 1 & -w_{12} & \cdots & -w_{1N} \\ 1 & 1 - w_{12} & \cdots & -w_{1N} \\ \vdots & \vdots & \ddots & \vdots \\ 1 & -w_{12} & \cdots & 1 - w_{1N} \end{vmatrix}. \quad (56)$$

Since $\sum_{i=1}^N w_{1i} = \mathbf{w}_1^T \mathbf{v}_1 = 1$, we have $\det(I - \mathbf{v}_1 \mathbf{w}_1^T) = 0$, which implies that the solution of (55) is not unique, i.e., \mathbf{r} is not unique. Note that \mathbf{r} contains the information of the relative state discrepancy with a predefined reference, and the discrepancy remains the same among different references. Since the term $\mathbf{v}_1 \mathbf{w}_1^T \mathbf{z}(0)$ is determined by the initial system condition, if $t \geq t_\epsilon$, the state discrepancy of $\mathbf{z}(t)$ is generated by \mathbf{m} . It follows that one of the solutions of (55) is given by

$$\mathbf{r} = \mathbf{m} - m_N \mathbf{1}, \quad (57)$$

where the N -th agent is taken as the predefined reference. Finally, setting $\mathbf{u} = \mathbf{u}_1 + \mathbf{u}_2$, and taking it into (11), we have

$$\mathbf{z}(t) = c\mathbf{1} \cdot t + (I - \mathbf{v}_1 \mathbf{w}_1^T) \mathbf{r} + \mathbf{v}_1 \mathbf{w}_1^T \mathbf{z}(0). \quad (58)$$

We then proof (13) by considering two enlightening cases. For $t \geq t_\epsilon$, if $c = 0$, then

$$\mathbf{z}(t) = (I - \mathbf{v}_1 \mathbf{w}_1^T) \mathbf{r} + \mathbf{v}_1 \mathbf{w}_1^T \mathbf{z}(0), \quad (59)$$

where $\mathbf{z}(t)$ reaches a stationary state, and the state discrepancy depends on \mathbf{r} with a predefined reference; if $\mathbf{r} = \mathbf{0}$, then

$$\mathbf{z}(t) = c\mathbf{1} \cdot t + \mathbf{v}_1 \mathbf{w}_1^T \mathbf{z}(0), \quad (60)$$

where $\mathbf{z}(t)$ updates at the constant rate $c\mathbf{1}$, and there is no state discrepancy. Inspired by the above analysis, we estimate $\mathbf{z}_0(t)$ by removing $\mathbf{z}_u(t)$ from $\mathbf{z}(t)$. Specifically, by differentiating (12), we have

$$\frac{d\mathbf{z}(t)}{dt} = c\mathbf{1}, \quad (61)$$

which is equivalent to the coefficient of the first term of $\mathbf{z}_u(t)$ in (8). If $t \geq t_\epsilon$, the global state discrepancy is reflected in \mathbf{r} and is equivalent to the entry discrepancy of the second term of $\mathbf{z}_u(t)$ in (8). Hence, the influence of \mathbf{z}_u is eliminable, and the estimated $\mathbf{z}_0(t)$ is given by

$$\hat{\mathbf{z}}_0(t) = \mathbf{z}(t) - c\mathbf{1} \cdot t - \mathbf{r}. \quad (62)$$

Since $\hat{\mathbf{z}}_0(k)$, the discrete expression of $\hat{\mathbf{z}}_0(t)$, represents the estimation of the data generated by the initial state, the solution to Φ_0 by using $\{\hat{\mathbf{z}}_0(k)\}$ is equivalent to the solution to the least square problem

$$\hat{P} = \arg \min_P \|\hat{Z}_{2:K+1} - P\hat{Z}_{1:K}\|_2^2. \quad (63)$$

To yield a unique solution of (63), it is necessary to guarantee that the rank of $\hat{Z}_{1:K}$ and $\hat{Z}_{2:K+1}$ is N . Hence, the minimum number of independent observations to obtain the optimal estimation is $N + 1$, and the solution of (63) is $\hat{P} =$

$\hat{Z}_{2:K+1} \hat{Z}_{1:K}^T (\hat{Z}_{1:K} \hat{Z}_{1:K}^T)^{-1}$. This concludes the proof. \square

C. Proof of Theorem 2

Proof. By Lemma 1, the estimation error is equivalent to the damping term of $\mathbf{z}_u(t)$, i.e.,

$$\psi_0(t) = \left\| \sum_{i=2}^N \frac{e^{-\lambda_i t}}{\lambda_i} \mathbf{v}_i \mathbf{w}_i^T \mathbf{u} \right\|_2. \quad (64)$$

Since λ_2 is the minimum non-zero eigenvalue, we have

$$\sum_{i=2}^N \frac{e^{-\lambda_i t}}{\lambda_i} \mathbf{v}_i \mathbf{w}_i^T \mathbf{u} \leq e^{-\lambda_2 t} \sum_{i=2}^N \frac{1}{\lambda_i} \mathbf{v}_i \mathbf{w}_i^T \mathbf{u} = e^{-\lambda_2 t} \mathbf{m}. \quad (65)$$

It follows that

$$\psi_0(t) \leq e^{-\lambda_2 t} \|\mathbf{m}\|_2. \quad (66)$$

When $\lambda_2 = \cdots = \lambda_N$, (66) takes the equal sign. Note that $e^{-\lambda_2 t}$ satisfies exponential decay, and $\|\mathbf{m}\|_2$ is a constant. Hence, the estimation error is bounded in a small range, and only impacts the initial converging period subtly. By Lemma 1, the damping terms of $\mathbf{z}(t)$ decrease to zero when $t > t_\epsilon$. It follows that $\lim_{t \rightarrow \infty} \psi_0(t) = 0$. \square

D. Proof of Theorem 3

Proof. We first prove the performance of empirical risk reformulation. By introducing $\hat{P}^s = P\hat{P}^{s-1}$ as an effective constraint on P , both \hat{Z}_0 and \mathcal{P}^s are used to solve the optimization problem. Define $f(\cdot)$ as the empirical risk value of an algorithm, given by the number of independent empirical functions. Larger $f(\cdot)$ means that the formulation of empirical risk contains more statistical information, enabling solving the corresponding optimization problem more accurately. For algorithm A_1 , the sum expression of its independent empirical functions is

$$\sum_{k=1}^{K-1} \alpha_k \|\hat{\mathbf{z}}_0(k+1) - P\hat{\mathbf{z}}_0(k)\|_2^2. \quad (67)$$

Hence, we have $f(A_1) = K - 1$. Considering the time horizon s , we have

$$\hat{\mathbf{z}}_0(k+s) = P^s \hat{\mathbf{z}}_0(k) + \mathbf{e}_0 s(k+s), \quad (68)$$

where $\mathbf{e}_0(k+s)$ is the estimation error vector. Note that the observation noise is independent zero-mean Gaussian random variable, thus, the entry of $\mathbf{e}_0(k+0)$ and $\mathbf{e}_0(k+s)$ are jointly independent. It follows that the additional empirical function of TO-TIA is independent to the empirical function of A_1 , and the sum expression of TO-TIA's empirical functions is

$$\sum_{k=1}^{K-1} \alpha_k \|\hat{\mathbf{z}}_0(k+1) - P\hat{\mathbf{z}}_0(k)\|_2^2 + \sum_{s=1}^{K-N} \|(P^s - P\hat{P}^{s-1})\|_F^2. \quad (69)$$

Then we have $f(\text{TO-TIA}) = 2K - N - 1$. Consequently, the empirical risk value of TO-TIA is larger than A_1 , i.e.,

$$f(A_1) < f(\text{TO-TIA}). \quad (70)$$

It follows that $\psi_m^* < \psi_m^1$, which concludes the proof of empirical risk reformulation.

We then prove the performance of weight design. The difference between TO-TIA, A_2 , and A_3 is the objective function of Φ_{1_b} , where the weighted cumulative information contained in the objective function determines the performance of the algorithm. To evaluate this error, we rewrite $\hat{\mathbf{z}}_0(k)$ as

$$\hat{\mathbf{z}}_0(k+1) = P\tilde{\mathbf{z}}_0(k) + \mathbf{e}_0(k+1). \quad (71)$$

Define $g(k+1)$ as the information value at time $k+1$, given by

$$\begin{aligned} g(k+1) &= \|\hat{\mathbf{z}}_0(k+1) - \hat{\mathbf{z}}_0(k)\|_2 \\ &= \|P(\tilde{\mathbf{z}}_0(k) - \tilde{\mathbf{z}}_0(k-1)) + \mathbf{e}_0(k+1) - \mathbf{e}_0(k)\|_2. \end{aligned} \quad (72)$$

On the one hand, by the consensus protocol, the state discrepancy of $\tilde{\mathbf{z}}_0(k)$ converges to zero asymptotically. On the other hand, the estimation error of $\tilde{\mathbf{z}}_0(k)$ is independent and decreases with k . Hence, we have

$$g(2) > \dots > g(K). \quad (73)$$

Then, define g_α as the weighted cumulative value, given by

$$g_\alpha = \sum_{k=2}^K \alpha_k g(k). \quad (74)$$

The weighted cumulative error of TO-TIA, A_2 , and A_3 is denoted as g_α^* , g_α^2 , and g_α^3 , respectively. It is easy to show that decreasing α_k generates the larger cumulative value than other weight design, i.e., $g_\alpha^* > g_\alpha^2 > g_\alpha^3$. Note that more valuable information leads to more accurate estimation, thus the relationship of estimation errors is contrary to the relationship of g_α^* , g_α^2 , and g_α^3 . This concludes the proof. \square

E. Proof of Proposition 1

Proof. First, we prove (27) by analyzing the function $h_1(j, k)$. Let $\Delta \mathbf{z}_0(k) = \mathbf{z}_0(k) - \mathbf{z}_0(k-1)$. By taking it into the first term of $h_1(j, k)$ and ignore the observation noise, we have

$$\left| \frac{\tilde{z}_j(k) - \tilde{z}_j(k-1)}{\tilde{z}_j(k-1) - \tilde{z}_j(k-2)} \right| = \left| \frac{\Delta z_{0_j}(k) + \varepsilon u_j(k-1)}{\Delta z_{0_j}(k-1)} \right|. \quad (75)$$

By Definition 1, in the discrete-time dynamics, the latent input is identifiable if

$$\left| \frac{\tilde{z}_j(k) - \tilde{z}_j(k-1)}{\varepsilon u_j(k-1)} \right| < l. \quad (76)$$

If $\mathbf{u}(k) = \mathbf{0}$, the latent input is unidentifiable. Thus, for $k < k_{u_q}$, inequation (76) does not hold, and we have

$$\left| \frac{\varepsilon u_j(k-1)}{\Delta z_{0_j}(k)} \right| < \frac{1}{l}. \quad (77)$$

Since the state discrepancy under the consensus protocol decreases with time, we have

$$\Delta z_{0_j}(k-1) \geq \Delta z_{0_j}(k). \quad (78)$$

Applying (77) and (78) to (75), we have

$$\begin{aligned} \left| \frac{\tilde{z}_j(k) - \tilde{z}_j(k-1)}{\tilde{z}_j(k-1) - \tilde{z}_j(k-2)} \right| &\leq \left| \frac{\Delta z_{0_j}(k) + \varepsilon u_j(k-1)}{\Delta z_{0_j}(k)} \right| \\ &= 1 + \left| \frac{\varepsilon u_j(k-1)}{\Delta z_{0_j}(k)} \right| < 1 + \frac{1}{l}, \end{aligned} \quad (79)$$

it follows that $h_1(j, k) < 0$. Once an agent is injected by input (i.e., $k = k_{u_q}$), (76) will not hold. Consequently, (79) will not hold and $h_1(j, k) \geq 0$. Therefore, for agent q , we have $h_1(q, k_{u_q}) < 0$ and $h_1(q, k_{u_q} + 1) \geq 0$. \square

F. Proof of Proposition 2

Proof. We prove this result by analyzing the function $h_2(j, k)$. Similar to (77), and by combining $\hat{P}^{(0)}$, a new discrete-time expression of (24) is

$$\left| \frac{\hat{P}_{[j]}^{(0)} \tilde{\mathbf{z}}(k-1) - \tilde{z}_j(k-1)}{\tilde{z}_j(k) - \hat{P}_{[j]}^{(0)} \tilde{\mathbf{z}}(k-1)} \right| < l. \quad (80)$$

For $j \in \mathcal{V}_u \setminus \{q\}$, if $k < k_{u_j}$, then (80) does not hold and $h_2(j, k) > 0$; if $k = k_{u_j}$, then agent j is injected by latent input. By Definition 1, $u_j(k_{u_j})$ is identifiable and (80) holds. Therefore, for $j \in \mathcal{V}_u \setminus \{q\}$, we have $h_2(j, k_{u_j}) > 0$ and $h_2(j, k_{u_j} + 1) \leq 0$. \square

G. Proof of Theorem 4

Proof. First, we prove (43). Define the set $\hat{\mathcal{Z}}_0^{(i)} = \{\hat{\mathbf{z}}_0^{(i)}(k)\}$, $\hat{\mathcal{U}}^{(i)} = \{\hat{\mathbf{u}}^{(i)}(k)\}$, and $e(\hat{\mathcal{X}}, \mathcal{X})$ as the estimation error of \mathcal{X} , given by

$$e(\hat{\mathcal{X}}, \mathcal{X}) = \frac{1}{|\mathcal{X}|} \sum_{\hat{\mathbf{x}} \in \hat{\mathcal{X}}, \mathbf{x} \in \mathcal{X}} \|\hat{\mathbf{x}} - \mathbf{x}\|_2. \quad (81)$$

Before the iteration, $\hat{P}^{(0)}$ is obtained without the estimation of \mathbf{u} , which is used to calculate $\hat{\mathcal{U}}^{(1)}$, and then $\hat{\mathcal{U}}^{(1)}$ is used to calculate $\hat{\mathcal{Z}}_0^{(1)}$. Based on the above analysis, and by $|\hat{\mathcal{Z}}_1| < |\hat{\mathcal{Z}}_0^{(1)}|$, we have

$$e(\hat{\mathcal{Z}}_0^{(1)}, \mathcal{Z}) < e(\hat{\mathcal{Z}}_1, \mathcal{Z}). \quad (82)$$

It follows that $\psi_m^* < \psi_m^1$. When $k > k_{u_j}$, (35) shows that $\hat{u}_j^{(i)}(k)$ is obtained by using $\hat{P}_{[j]}^{(i-1)}$, then we have

$$\begin{aligned} \hat{u}_j^{(i)}(k_{u_j}) &= \frac{1}{\varepsilon} (\tilde{z}_j(k_{u_j}) - \hat{P}_{[j]}^{(i-1)} \tilde{z}_j(k_{u_j} - 1)) \\ &= \frac{1}{\varepsilon} [\tilde{z}_j(k_{u_j}) - P_{[j]}^{(i-1)} \tilde{z}_j(k_{u_j} - 1) - e_p^{(i)}(k_{u_j})] \\ &= u_j(k_{u_j}) - \frac{1}{\varepsilon} \psi_s^{p(i)}(k_{u_j}), \end{aligned} \quad (83)$$

where $\psi_s^{p(i)}(k_{u_j})$ is the error generated by $\hat{P}^{(i-1)}$. Note that (37) implies that the error of $\hat{\mathbf{z}}_0^{(i)}(k_{u_j})$ is generated by the error of $\hat{u}_j^{(i)}(k)$. Hence, we have

$$\begin{aligned} \hat{\mathbf{z}}_0^{(i)}(k_{u_j}) &= \tilde{\mathbf{z}}_0(k_{u_j}) - \varepsilon \hat{u}_j^{(i)}(k_{u_j}) \\ &= \tilde{\mathbf{z}}_0(k_{u_j}) - \varepsilon u_j(k_{u_j}) + \psi_s^{p(i)}(k_{u_j}). \end{aligned} \quad (84)$$

Therefore, k_{u_j} is the key time to predict $\hat{Z}_0^{(i)}$, and $\psi_s^{p(i)}(k_{u_j})$ determines the accuracy of the next iteration. Then we have

$$e(\hat{U}^{(2)}, \mathcal{U}) < e(\hat{U}^{(1)}, \mathcal{U}), \quad (85)$$

which is equivalent to $\psi_\theta^{(2)} < \psi_\theta^{(1)}$, and implies that $\psi_m^{(2)} < \psi_m^{(1)}$. Consequently, for the whole iteration, we have

$$\begin{cases} \psi_m^{(i+1)} < \psi_m^{(i)}, \\ \psi_\theta^{(i+1)} < \psi_\theta^{(i)}. \end{cases} \quad (86)$$

Second, we prove the algorithm complexity of IE-TIA. Before the iterative estimation, since the topology inference is performed once to obtain an original estimated P , the initialization complexity is $O(1)$. In the iteration stage, the stopping criterion (39) does not hold, i.e., $\psi_d^{(i)} \geq \delta_d$ in the i -th iteration. Hence, the number of iterations required is $O(\frac{\psi_m^{(0)}}{\delta_m})$. As a result of the structure of IE-TIA, the algorithm complexity amounts to the iteration complexity.

Finally, we prove the third conclusion by analyzing the reason that caused the topology inference error. Define $Er(\cdot)$ as the error induced by (\cdot) . By (35), the error of $\hat{\mathbf{u}}^{(i)}(k)$ is induced by the error of $\hat{P}^{(i-1)}$. Hence, we have

$$\hat{\mathbf{u}}^{(i)}(k) = \mathbf{u}(k) + Er(\hat{P}^{(i-1)}). \quad (87)$$

Based on (37), if $k = k_{u_j}$, the error of $\hat{z}_{\varphi_j}^{(i)}(k)$ is induced by the error of $\hat{\mathbf{u}}^{(i)}(k)$; if $k > k_{u_j}$, the error of $\hat{z}_{\varphi_j}^{(i)}(k)$ is induced by the error of $\hat{P}^{(i-1)}$. Thus, (37) is rewritten as

$$\hat{z}_{\varphi_j}^{(i)}(k) = \begin{cases} z_{\varphi_j}(k), & \text{if } k < k_{u_j}, \\ z_{\varphi_j}(k) + Er(\hat{\mathbf{u}}^{(i)}(k)), & \text{if } k = k_{u_j}, \\ z_{\varphi_j}(k) + Er(\hat{P}^{(i-1)}), & \text{if } k > k_{u_j}. \end{cases} \quad (88)$$

By (87), we have

$$Er(\hat{\mathbf{u}}^{(i)}(k)) = Er(\mathbf{u}(k)) + Er(\hat{P}^{(i-1)}) = Er(\hat{P}^{(i-1)}), \quad (89)$$

and by taking it into (88), the global form of $\hat{z}_{\varphi_j}^{(i)}(k)$ is

$$\hat{z}_{\varphi}^{(i)}(k) = \mathbf{z}_\varphi(k) + Er(\hat{P}^{(i-1)}). \quad (90)$$

Since $\hat{P}^{(i)}$ is obtained by using $\{\hat{z}_{\varphi_j}^{(i)}(k)\}$, the error of $\hat{P}^{(i)}$ is induced by the error of $\hat{z}_{\varphi}^{(i)}(k)$. Hence, we have

$$\begin{aligned} Er(\hat{P}^{(i)}) &= Er(\hat{\mathbf{z}}_\varphi^{(i)}(k)) \\ &= Er(\mathbf{z}_\varphi(k)) + Er(P^{(i-1)}) \\ &= Er(P^{(i-1)}). \end{aligned} \quad (91)$$

Consequently, the final solution satisfies

$$Er(\hat{P}^{(i_t)}) = Er(\hat{P}^{(i_t-1)}) = \dots = Er(\hat{P}^{(0)}). \quad (92)$$

Recalling that $\hat{P}^{(0)}$ is obtained by using \tilde{Z}_1 , which consists of the observations before time k_{u_q} . By Theorem 1, if $k_{u_q} \geq N + 1$, then the initial estimation of P in the least square sense is optimal. According to (92), the final estimation error is ultimately generated by the initially estimated P . It follows that the final estimation of P in the least square sense is optimal, given by

$$\hat{P}^{(i_t)} = \hat{Z}_\varphi^{(i_t)2:K} (\hat{Z}_\varphi^{(i_t)1:K-1})^T (\hat{Z}_\varphi^{(i_t)1:K-1} (\hat{Z}_\varphi^{(i_t)1:K-1})^T)^{-1}. \quad (93)$$

Since IE-TIA decreases the estimation error with iteration

continuously, we have

$$\lim_{i \rightarrow \infty} \psi_\theta^{(i)} = \psi_m^{(i)} = 0. \quad (94)$$

It follows that

$$\lim_{i \rightarrow \infty} \hat{\mathbf{z}}_\varphi^{(i)}(k) = \mathbf{z}_\varphi(k). \quad (95)$$

Consequently, if $i \rightarrow \infty$, (93) is equivalent to (42), i.e.,

$$\lim_{i \rightarrow \infty} \hat{P}^{(i)} = P^*. \quad (96)$$

This concludes the proof. \square

REFERENCES

- [1] Q. Jiao, Y. Li, J. He, and L. Shi, "Topology inference for consensus-based cooperation under time-invariant latent input," submitted to *Proc. IEEE ACC*, 2021.
- [2] R. Olfati-Saber and R. M. Murray, "Consensus problems in networks of agents with switching topology and time-delays," *IEEE Trans. Autom. Control*, vol. 49, no. 9, pp. 1520–1533, 2004.
- [3] R. Olfati-Saber, J. A. Fax, and R. M. Murray, "Consensus and cooperation in networked multi-agent systems," in *Proc. IEEE*, vol. 95, no. 1, pp. 215–233, 2007.
- [4] P. Yang, R. A. Freeman, and K. M. Lynch, "Multi-agent coordination by decentralized estimation and control," *IEEE Trans. Autom. Control*, vol. 53, no. 11, pp. 2480–2496, 2008.
- [5] D. A. Burbano-L, R. Freeman, and K. Lynch, "Inferring the network topology of interconnected nonlinear units with diffusive couplings," in *Proc. IEEE ACC*, pp. 3398–3403, 2018.
- [6] S. Sardellitti, S. Barbarossa, and P. D. Lorenzo, "Graph topology inference based on sparsifying transform learning," *IEEE Trans. Signal Process.*, 2019.
- [7] S. Segarra, A. G. Marques, M. Goyal, and S. Rey-Escudero, "Network topology inference from input-output diffusion pairs," in *Proc. IEEE Statistical Signal Processing Workshop*, pp. 508–512, 2018.
- [8] X. Dong, D. Thanou, M. Rabbat, and P. Frossard, "Learning graphs from data: A signal representation perspective," *IEEE Signal Processing Magazine*, vol. 36, no. 3, pp. 44–63, 2019.
- [9] S. Shahrampour and V. M. Preciado, "Topology identification of directed dynamical networks via power spectral analysis," *IEEE Trans. Autom. Control*, vol. 60, no. 8, pp. 2260–2265, 2014.
- [10] S. Segarra, A. G. Marques, G. Mateos, and A. Ribeiro, "Network topology inference from spectral templates," *IEEE Trans. Signal and Information Processing over Networks*, vol. 3, no. 3, pp. 467–483, 2017.
- [11] D. Hayden, Y. Yuan, and J. Gonçalves, "Network identifiability from intrinsic noise," *IEEE Trans. Autom. Control*, vol. 62, no. 8, pp. 3717–3728, 2016.
- [12] M. Timme and J. Casadiego, "Revealing networks from dynamics: an introduction," *Journal of Physics A Mathematical and Theoretical*, vol. 47, no. 34, p. 343001, 2014.
- [13] F. Lu, M. Zhong, S. Tang, and M. Maggioni, "Nonparametric inference of interaction laws in systems of agents from trajectory data," in *Proc. the National Academy of Sciences*, vol. 116, no. 29, pp. 14424–14433, 2019.
- [14] A. Santos, V. Matta, and A. H. Sayed, "Consistent tomography over diffusion networks under the low-observability regime," in *Proc. IEEE International Symposium on Information Theory*, pp. 1839–1843, 2018.
- [15] P. Geiger, K. Zhang, B. Schoelkopf, M. Gong, and D. Janzing, "Causal inference by identification of vector autoregressive processes with hidden components," in *International Conf. Machine Learning*, pp. 1917–1925, 2015.
- [16] Y. Shen, B. Baingana, and G. B. Giannakis, "Topology inference of directed graphs using nonlinear structural vector autoregressive models," in *Proc. IEEE International Conf. Acoustics, Speech and Signal Processing*, pp. 6513–6517, 2017.
- [17] S. P. Chepuri, S. Liu, G. Leus, and A. O. Hero, "Learning sparse graphs under smoothness prior," in *Proc. IEEE International Conf. Acoustics, Speech and Signal Processing*, pp. 6508–6512, 2017.
- [18] S. Kar and J. M. F. Moura, "Consensus + innovations distributed inference over networks: Cooperation and sensing in networked systems," *IEEE Signal Processing Magazine*, vol. 30, no. 3, pp. 99–109, 2013.
- [19] C. Zhao, J. He, P. Cheng, and J. Chen, "Consensus-based energy management in smart grid with transmission losses and directed communication," *IEEE Trans. Smart Grid*, vol. 8, no. 5, pp. 2049–2061, 2016.

- [20] K. F. E. Tsang, M. Huang, K. H. Johansson, and L. Shi, "Sparse linear injection attack on multi-agent consensus control systems," *IEEE Control Systems Letters*, vol. 5, no. 2, pp. 665–670, 2020.
- [21] K. Kikuchi, A. Cetinkaya, T. Hayakawa, and H. Ishii, "Stochastic communication protocols for multi-agent consensus under jamming attacks," in *Proc. IEEE CDC*, pp. 1657–1662, 2017.
- [22] A. H. Soliman and A. A. H. Mantawy, "Modern optimization techniques with applications in electric power systems," *Springer Science and Business Media*, 2011.
- [23] W. Ren and R. W. Beard, *Distributed consensus in multi-vehicle cooperative control*, vol. 27, Springer, 2008.
- [24] Y. Yuan, X. Tang, W. Zhou, W. Pan, X. Li, H.-T. Zhang, H. Ding, and J. Goncalves, "Data driven discovery of cyber physical systems," *Nature communications*, vol. 10, no. 1, pp. 1–9, 2019.
- [25] F. L. Lewis, H. Zhang, K. Hengster-Movric, and A. Das, *Cooperative control of multi-agent systems: optimal and adaptive design approaches*. Springer Science and Business Media, 2013.
- [26] Y. Mao and E. Akyol, "On network topology inference of social networks," in *Proc. IEEE Annual Allerton Conf. Communication, Control and Computing*, pp. 804–809, 2019.
- [27] D. L. Donoho, "For most large underdetermined systems of linear equations the minimal l_1 -norm solution is also the sparsest solution," *Communications on Pure and Applied Mathematics: A Journal Issued by the Courant Institute of Mathematical Sciences*, vol. 59, no. 6, pp. 797–829, 2006.
- [28] J. Friedman, T. Hastie, and R. Tibshirani, "Sparse inverse covariance estimation with the graphical lasso," *Biostatistics*, vol. 9, no. 3, pp. 432–441, 2008.
- [29] Y. Shen, G. B. Giannakis, and B. Baingana, "Nonlinear structural vector autoregressive models with application to directed brain networks," *IEEE Trans. Signal Process.*, vol. 67, no. 20, pp. 5325–5339, 2019.
- [30] S. J. Kim, K. Koh, and M. Lustig, "An interior-point method for large-scale '1-regularized least squares," *IEEE Journal of Selected Topics in Signal Process.*, vol. 1, no. 4, pp. 606–617, 2008.
- [31] F. Ding and T. Chen, "Hierarchical least squares identification methods for multivariable systems," *IEEE Trans. Autom. control*, vol. 50, no. 3, pp. 397–402, 2005.
- [32] M. Verhaegen and V. Verdult, *Filtering and system identification: a least squares approach*. Cambridge University Press, 2007.
- [33] A. Sandryhaila and J. M. F. Moura, "Discrete signal processing on graphs," *IEEE Trans. Signal Process.*, vol. 61, no. 7, pp. 1644–1656, 2013.
- [34] Y. Zhu, M. T. Schaub, A. Jadbabaie, and S. Segarra, "Network inference from consensus dynamics with unknown parameters," *IEEE Trans. Signal and Information Processing over Networks*, vol. 6, pp. 300–315, 2020.
- [35] X. Dong, D. Thanou, P. Frossard, and P. Vandergheynst, "Learning laplacian matrix in smooth graph signal representations," *IEEE Trans. Signal Process.*, vol. 64, no. 23, pp. 6160–6173, 2016.
- [36] B. Pasdeloup, V. Gripon, G. Mercier, D. Pastor, and M. G. Rabbat, "Characterization and inference of graph diffusion processes from observations of stationary signals," *IEEE Trans. Signal and Information Processing over Networks*, vol. PP, no. 3, pp. 1–1, 2018.
- [37] H. E. Egilmez, E. Pavez, and A. Ortega, "Graph learning from filtered signals: Graph system and diffusion kernel identification," *IEEE Trans. Signal and Information Processing over Networks*, vol. 5, no. 2, pp. 360–374, 2018.
- [38] D. Thanou, X. Dong, D. Kressner, and P. Frossard, "Learning heat diffusion graphs," *IEEE Trans. Signal and Information Processing over Networks*, vol. 3, no. 3, pp. 484–499, 2017.
- [39] R. Shafipour, S. Segarra, A. G. Marques, and G. Mateos, "Network topology inference from non-stationary graph signals," in *Proc. IEEE International Conference on Acoustics, Speech and Signal Processing*, pp. 5870–5874, 2017.
- [40] S. P. Chepuri, S. Liu, G. Leus, and A. O. Hero, "Learning sparse graphs under smoothness prior," in *Proc. IEEE International Conference on Acoustics*, 2017.
- [41] X. Dong, D. Thanou, P. Frossard, and P. Vandergheynst, "Learning laplacian matrix in smooth graph signal representations," *IEEE Trans. Signal Processing*, vol. 64, no. 23, pp. 6160–6173, 2016.
- [42] M. Schmidt and H. Lipson, "Distilling free-form natural laws from experimental data," *Science*, vol. 324, no. 5923, pp. 81–85, 2009.
- [43] Y. H. Chang and C. Tomlin, "Data-driven graph reconstruction using compressive sensing," in *Proc. IEEE CDC*, pp. 1035–1040, 2012.
- [44] M. Nabi-Abdolyousefi and M. Mesbahi, "Network identification via node knockout," *IEEE Trans. Autom. Control*, vol. 57, no. 12, pp. 3214–3219, 2012.
- [45] D. A. Burbano-L, R. Freeman, and K. Lynch, "Inferring the network topology of interconnected nonlinear units with diffusive couplings," in *Proc. IEEE ACC*, pp. 3398–3403, 2018.
- [46] S. Shahrapour and V. M. Preciado, "Reconstruction of directed networks from consensus dynamics," in *Proc. IEEE ACC*, pp. 1685–1690, 2013.
- [47] M. Nabi-Abdolyousefi, M. Fazel, and M. Mesbahi, "A graph realization approach to network identification," in *Proc. IEEE CDC*, pp. 4642–4647, 2012.
- [48] V. Matta and A. H. Sayed, "Consistent tomography under partial observations over adaptive networks," *IEEE Trans. Information Theory*, vol. 65, no. 1, pp. 622–646, 2018.
- [49] D. Materassi and M. V. Salapaka, "On the problem of reconstructing an unknown topology via locality properties of the wiener filter," *IEEE Trans. Autom. Control*, vol. 57, no. 7, pp. 1765–1777, 2012.
- [50] Y. Ye, G. B. Stan, S. Warnick, and J. Goncalves, "Robust dynamical network structure reconstruction," *Automatica*, vol. 47, no. 6, pp. 1230–1235, 2011.
- [51] Wei Ren and R. W. Beard, "Consensus seeking in multiagent systems under dynamically changing interaction topologies," *IEEE Trans. Autom. Control*, vol. 50, no. 5, pp. 655–661, 2005.
- [52] W. Ren, "Multi-vehicle consensus with a time-varying reference state," *Systems and Control Letters*, vol. 56, no. 7, pp. 474 – 483, 2007.
- [53] S. Hassan-Moghaddam, N. K. Dhingra, and M. R. Jovanović, "Topology identification of undirected consensus networks via sparse inverse covariance estimation," in *Proc. IEEE CDC*, pp. 4624–4629, 2016.
- [54] G. Mateos, S. Segarra, A. G. Marques, and A. Ribeiro, "Connecting the dots: Identifying network structure via graph signal processing," *IEEE Signal Processing Magazine*, vol. 36, no. 3, pp. 16–43, 2019.

Qing Jiao (S'19) received the B.E. degree in the Department of Automation from Xiamen University, Xiamen, China, in 2019.

She is currently working toward the Ph.D. degree with the Department of Automation, Shanghai Jiaotong University, Shanghai, China. She is a member of Intelligent of Wireless Networking and Cooperative Control group. Her research interests include multi-robot cooperative control and topology inference in multi-agent networks.

Yushan Li (S'19) received the B.E. degree in School of Artificial Intelligence and Automation from Huazhong University of Science and Technology, Wuhan, China, in 2018.

He is currently working toward the Ph.D. degree with the Department of Automation, Shanghai Jiaotong University, Shanghai, China. He is a member of Intelligent of Wireless Networking and Cooperative Control group. His research interests include robotics, security of cyber-physical system, and distributed computation and optimization in multi-agent networks.

Jianping He (M'15-SM'19) is currently an associate professor in the Department of Automation at Shanghai Jiao Tong University. He received the Ph.D. degree in control science and engineering from Zhejiang University, Hangzhou, China, in 2013, and had been a research fellow in the Department of Electrical and Computer Engineering at University of Victoria, Canada, from Dec. 2013 to Mar. 2017. His research interests mainly include the distributed learning, control and optimization, security and privacy in network systems.

Dr. He serves as an Associate Editor for IEEE Open Journal of Vehicular Technology and KSII Trans. Internet and Information Systems. He was also a Guest Editor of IEEE TAC, International Journal of Robust and Nonlinear Control, etc. He was the winner of Outstanding Thesis Award, Chinese Association of Automation, 2015. He received the best paper award from IEEE WCSP'17, the best conference paper award from IEEE PESGM'17, and was a finalist for the best student paper award from IEEE ICCA'17.

Ling Shi (SM'17) received the B.S. degree in electrical and electronic engineering from Hong Kong University of Science and Technology, Kowloon, Hong Kong, in 2002 and the Ph.D. degree in Control and Dynamical Systems from California Institute of Technology, Pasadena, CA, USA, in 2008.

He is currently an associate professor at the Department of Electronic and Computer Engineering, and the associate director of the Robotics Institute, both at the Hong Kong University of Science and Technology. His research interests include cyber-physical systems security, networked control systems, sensor scheduling, event-based state estimation and exoskeleton robots. He is a senior member of IEEE. He served as an editorial board member for The European Control Conference 2013-2016. He was a subject editor for International Journal of Robust and Nonlinear Control (2015-2017). He has been serving as an associate editor for IEEE Transactions on Control of Network Systems from July 2016, and an associate editor for IEEE Control Systems Letters from Feb 2017. He also served as an associate editor for a special issue on Secure Control of Cyber Physical Systems in the IEEE Transactions on Control of Network Systems in 2015-2017. He served as the General Chair of the 23rd International Symposium on Mathematical Theory of Networks and Systems (MTNS 2018). He is a member of the Young Scientists Class 2020 of the World Economic Forum (WEF).